Final Technical Report

Contract:
1305M221PNCNL0276

Title:
Modernization Modeling Support - Euler Pole Parameters (EPP) & Strain Rate Modeling

Principal Investigator:
Corné Kreemer – University of Nevada, Reno

Summary

This report presents an analysis of the 3D velocity field for intraplate North America. The task was to model the deformation field from GPS-derived horizontal velocities and obtain parameters that describe the net-rotation of this deforming plate. These parameters are very stable against some modeling choices. We then found a set of 16 station velocities spread across the plate, which, when modeled with a rigid plate rotation, yield an Euler pole (1.86°S, 86.04°W, 0.2050°/Myr), which is nearly indistinguishable from the derived net-rotation. For completeness we also present the vertical land motion for intraplate North America.

Approach

Data

We considered all GPS time-series available through the Nevada Geodetic Laboratory (Blewitt et al., 2018). Those data are processed with the GipsyX Precise-Point-Positioning in the IGS14 reference frame. Processing details can be found in Kreemer et al. (2020) as well as here: http://geodesy.unr.edu/gps/ngl.acn.txt. The original RINEX data come from a wide array of data providers. Most data come from the National Geodetic Survey CORS network, but supplemented most notably by data from National Resources Canada (including their campaign Canadian Base Network), G-NET in Greenland, numerous state agencies, the Network of the Americas, and stations in northwestern Iceland.

We corrected the position time-series for non-tidal ocean loading and non-tidal atmospheric loading; this mostly affects the precision of the vertical rates. We also correct the time-series for surface deformation induced by hydrological loading derived from GRACE mascons. This can affect the precision and rate of vertical time-series, but also of horizontal ones, as was shown for stations around the Great Lakes responding to lake (un)loading (Argus et al., 2020).

We considered all position estimates between Jan 1, 2005 and Dec 31, 2022 with a minimum time-series span of 875 days (~2.4 years) and located within the polygon provided as an electronic supplement. Offsets were estimated at times of known equipment changes or at times otherwise observed to have an offset. This was done as part of fitting a station motion model to the position time-series, that also included an annual and semi-annual signal. From the residual time-series, we removed outliers using a 3-sigma limit (defined using robust statistics) in an iterative process until no outlier remains. Stations with significant non-linear/erratic motion (which often can be attributed to local hydrology) were excluded, as were stations in the middle of Greenland Icesheet, and stations possibly affected by mass loading variations at terminal glacier outliers (HEL2, KAGA, KUAQ, RINK, SRMP). Finally, from the offset-corrected time-series we derive a rate and uncertainty with the MIDAS algorithm (Blewitt et al., 2016).

The resulting 4274 velocities are listed in the electronic supplement. Figure 1 shows the station locations, color-coded by the length of observation. There were a few stations collocated with others (defined as being <1 m apart); in those cases their velocities were averaged for the purpose of the 3D deformation modeling. This means that we actually used 4256 velocities for the modeling (provided in a separate file).

Strain Rate Modeling

We then took the 4256 horizontal velocities to estimate a strain rate and rotation rate field using the MELD algorithm (Kreemer et al., 2020, 2018). Model parameters, are calculated on a grid of points; we consider either 0.5° or 1° grid spacing. The algorithm requires as input a minimum number of triangles for each grid point from which to derive multivariate median parameters. We consider either N=56 or 120 triangles, which can in theory be formed by 8 or 10 GPS points, respectively. In reality, more GPS points need to be considered, because we do exclude triangles that are too small or too skinny. This requirement is set by the σ_{max} parameter. We specify σ_{max} with the requirement that the typical noise in the data (defined here by the median standard deviation in the horizontal velocities, 0.21 mm/yr) does not translate into a strain rate higher than 10^{-9}/yr. This translates to σ_{max} = 5.72 x 10^{-9}/yr, and the area of the corresponding triangle has an area equivalent to a circle with ~92 km radius. We consider this our best spatial resolution. Evidently, if we would be satisfied with noise leaking into strain rates as high as, for example, 2 x 10^{-9}/yr, we would double σ_{max} and the corresponding spatial resolution would be ~46 km.

The MELD FORTRAN code (and associated Delaunay triangulation code (Renka, 1997)) are provided as electronic supplements.

Vertical land motion Imaging

While not important for the Euler pole estimation, for completeness we also image the vertical land motion (VLM). Combining the VLM with the dilatational strain rate field, might facilitate explorations of the origin of the signals. The VLM observations are shown in Figure 4. We use the Robust Network Imaging technique presented by Kreemer et al. (2020), where the details can be found.

Results

We focus here on the MELD model with N=56, σ_{max} = 5.72 x 10^{-9}/yr and sampled at 0.5° grid, which are the input parameters we recommend. For this model we present the intraplate velocity field in Figure 2 (this is the IGS14 velocity field minus the velocities predicted by the net-rotation of the plate). The velocity pattern, dominated by far-field points moving towards the former ice-sheet at 1-2 mm/yr, is similar to what was presented by Kreemer et al. (2018). As far as the strain rate field is concerned, the dominant features can be found in the dilatational rate field (Figure 3). Large-scale features that were previously identified as GIA-related are still there (Kreemer et al., 2018). Some significant smaller-scale features are also appearing, most notably extension in the Permian Basin (West Texas and SE New Mexico), southwest Texas, and east of New Madrid, and contraction near the Meers fault in southern Oklahoma.

The imaged vertical land motion is shown in Figure 5. The field is dominated by uplift of areas underneath the former ice-sheet and subsidence of the area just to the south.

Euler Pole Estimation

The main result from the MELD modeling that is applicable to this project is that one can estimate the net-rotation of the area encompassed by the network. This net-rotation is

estimated as the average area-weighted rotation vector when considering the (average) rotation vectors at all grid points for which model parameters were derived. Table 1 gives the rotation vector and associated pole location for different models (grid spacing, N and σ_{max}). Generally, the Euler pole parameters are extremely close.

Table 1 *– Net-rotation vector and corresponding pole for strain rate models with different parameter choices. Rotation rate (ω) given in °/Myr.*

	ω(x)	ω(y)	ω(z)	σ ω(x)	σ ω(y)	σ ω(z)	Lat.	Long.	ω
0.5°,N56,σmax=5.72	0.0142	-0.2044	-0.0066	0.0080	0.0136	0.0117	-1.88	-85.99	0.2049
1°,N56,σmax=5.72	0.0143	-0.2043	-0.0067	0.0081	0.0140	0.0121	-1.88	-86.00	0.2049
0.5°,N56,σmax=11.44	0.0144	-0.2045	-0.0075	0.0083	0.0165	0.0141	-2.11	-85.96	0.2051
1°,N56,σmax=11.44	0.0144	-0.2044	-0.0076	0.0085	0.0199	0.0166	-2.13	-85.96	0.2050
1°,N120,σmax=5.72	0.0146	-0.2041	-0.0067	0.0083	0.0137	0.0114	-1.88	-85.92	0.2048

Next, we searched for a set of stations that, when taking their velocities to estimate an Euler pole (without assumption of internal deformation) yields a pole as close as possible to the net-rotation poles derived above. For this, and after much trial-and-error, we chose 16 stations that are relatively even spaced and have (relatively) stable, and ongoing, time-series. The most important selection criterion is that you need stations that evenly sample different parts of the intraplate deformation. The east-west coverage is particularly important given that the Euler pole is located south of the plate. The set of stations is listed in Table 2 and shown in Figure 2, and the resulting rotation vector and Euler pole are in Table 3 and 4, resp.

Table 2 *– Stations that can be used to estimate a rotation vector that best estimates North America's net-rotation estimated from the strain rate modeling*

Station	Latitude	Longitude
BAKE	64.3178	-96.0023
BRSG	32.3704	-64.6964
FLRS	39.4538	-31.1264
HCES	36.3326	-89.1718
ISAF	66.0736	-23.1195
JGBL	82.2088	-31.0042
LAUD	26.1962	-80.1731
NRC1	45.4542	-75.6238
P042	42.0515	-104.9106
PICL	51.4798	-90.1620
QAQ1	60.7153	-46.0478
QIKI	67.5593	-64.0337
SCH2	54.8321	-66.8326
SG27	71.3229	-156.6103
STJO	47.5952	-52.6777
UCAL	51.0800	-114.1339

Table 3 *– IGS14 rotation vector and standard deviations and correlation coefficients (cc) estimated from velocities at sites listed in Table 2. Rotation rate (ω) given in °/Myr.*

ω(x)	ω(y)	w(z)	σ ω(x)	σ ω(y)	σ ω(z)	cc(x,y)	cc(x,z)	cc(y,z)
0.0142	-0.2044	-0.0066	0.0004	0.0006	0.0008	-0.2574	0.2998	-0.7373

Table 4 *– IGS14 Euler pole estimated from velocities at sites listed in Table 2. a and b are semi major and minor axes, resp. Rotation rate (ω) given in °/Myr.*

Latitude	Longitude	ω	σ **ω**	*a*	*b*	Azi. *a*
-1.86°	-86.04°	0.2050	0.0006	0.32°	0.13°	58.9°

Bibliography

Argus, D.F., Ratliff, B., DeMets, C., Borsa, A.A., Wiese, D.N., Blewitt, G., Crowley, J.W., Martens, H.R., Kreemer, C., Landerer, F.W., 2020. Rise of Great Lakes Surface Water, Sinking of the Upper Midwest of the United States, and Viscous Collapse of the Forebulge of the Former Laurentide Ice Sheet. J. Geophys. Res. Solid Earth 125, e2020JB019739. https://doi.org/10.1029/2020JB019739

Blewitt, G., Hammond, W.C., Kreemer, C., 2018. Harnessing the GPS data explosion for interdisciplinary science. Eos 99. https://doi.org/10.1029/2018EO104623

Blewitt, G., Kreemer, C., Hammond, W.C., Gazeaux, J., 2016. MIDAS robust trend estimator for accurate GPS station velocities without step detection. J. Geophys. Res. Solid Earth 121, 2054–2068. https://doi.org/10.1002/2015JB012552

Kreemer, C., Blewitt, G., Davis, P.M., 2020. Geodetic evidence for a buoyant mantle plume beneath the Eifel volcanic area, NW Europe. Geophys. J. Int. 222, 1316–1332. https://doi.org/10.1093/gji/ggaa227

Kreemer, C., Hammond, W.C., Blewitt, G., 2018. A robust estimation of the 3-D intraplate deformation of the North American plate from GPS. J. Geophys. Res.-Solid Earth 123, 4388–4412. https://doi.org/10.1029/2017JB015257

Renka, R.J., 1997. Algorithm 772: STRIPACK: Delaunay triangulation and Voronoi diagram on the surface of a sphere. ACM Trans Math Softw 23, 416–434. https://doi.org/10.1145/275323.275329

Electronic Supplements:

GPS_velocities.txt :	lon, lat, vlon_IGS14, vlat_IGS14, vup_IGS14, σ_vlon_IGS14, σ_vlat_IGS14, σ_vup_IGS14, vlon_intraplate, vlat_intraplate
GPS_velocities_combined.txt :	lon, lat, vlon_IGS14, vlat_IGS14, vup_IGS14, σ_vlon_IGS14, σ_vlat_IGS14, σ_vup_IGS14, vlon_intraplate, vlat_intraplate
NA.alt.rev.gmt :	North American polygon
residuals.gmt :	Residual velocities from MELD model (0.5°,N56,σ_{max}=5.72) – lon, lat, vlon, vlat, σ_vlon, σ_vlat, corr.coef., name
ave_vel_pred_grid.gmt :	Predicted horiz. IGS14 velocities at 0.5° grid; lon,lat,vlon,vlat
VLM_grid :	Imaged vert. IGS14 velocities at 0.5° grid; lon, lat, v, σ
MELD.f90	MELD.f90
delaunay.f90	delaunay.f90
determine_euler_pole_gmt.f	determine_euler_pole_gmt.f (code to calculate EPP)
llh.euler	stations listed in Table 2
run_EPP	UNIX C-shell script to run determine_euler_pole_gmt
run_MELD	UNIX C-shell script to run MELD

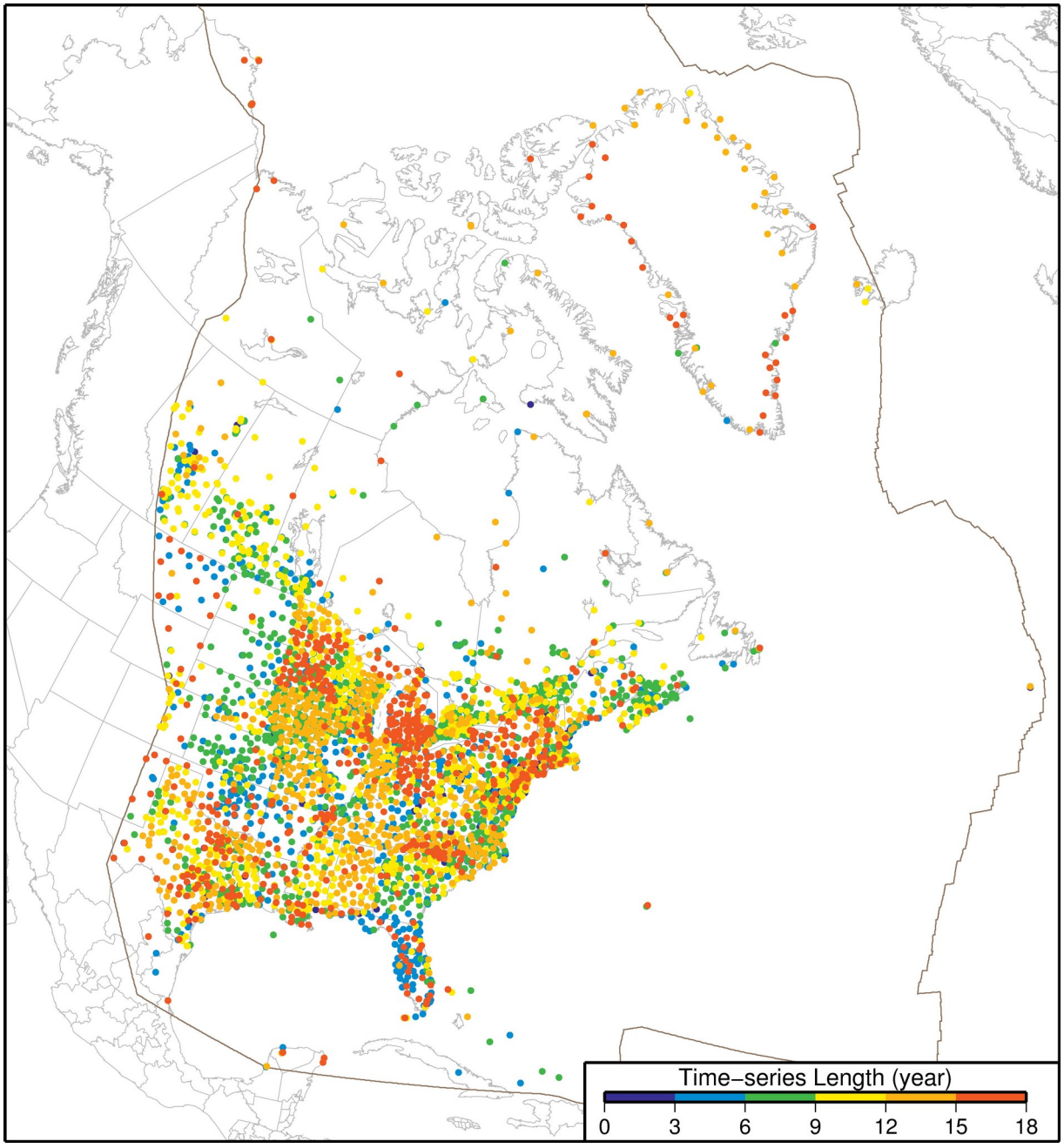

Figure 1 *– Locations and length of time-series of all 4274 stations used within the given polygon (brown line).*

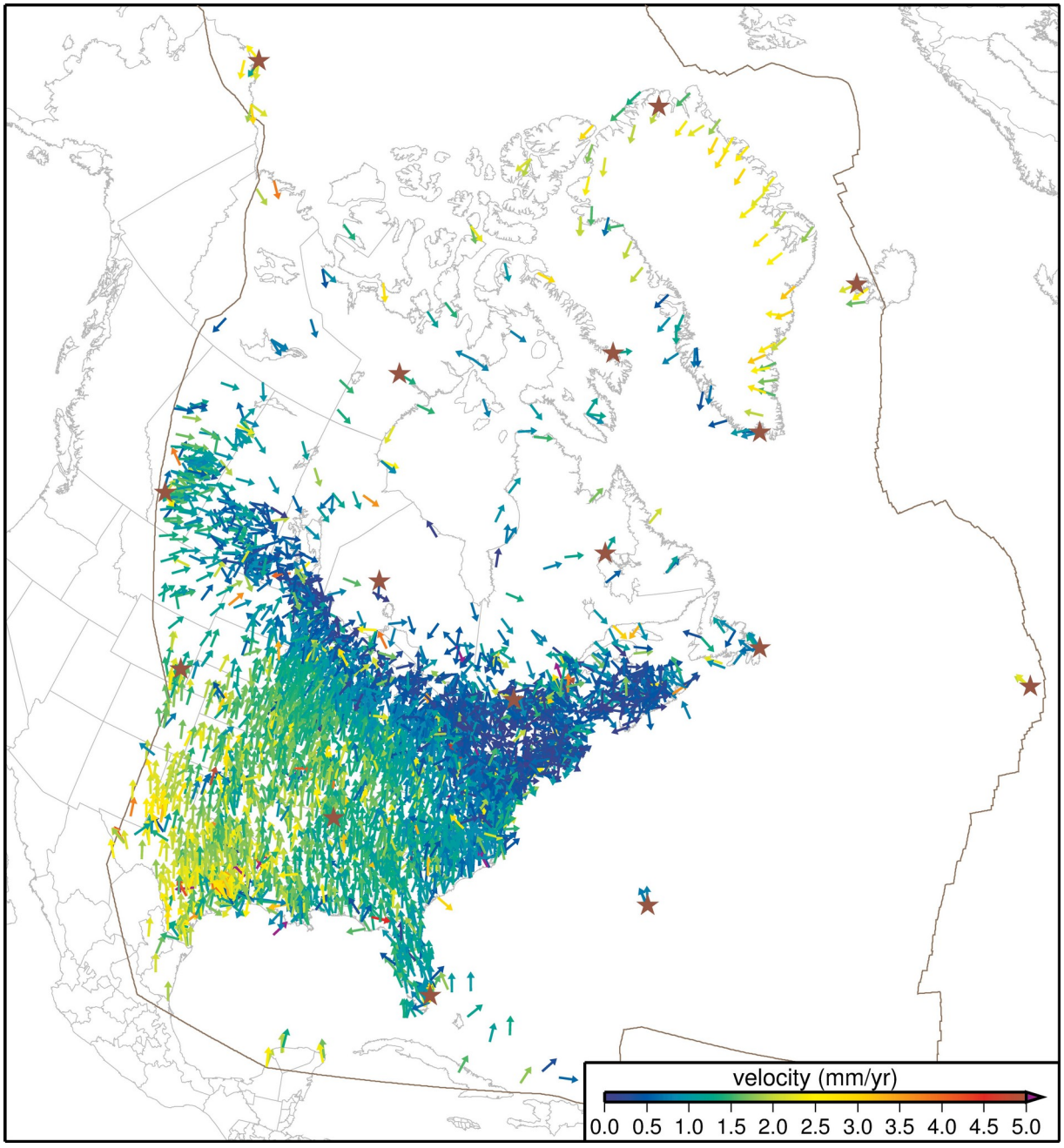

Figure 2 *– Intraplate velocities; i.e., IGS14 velocities minus those predicted by the net-rotation of the area captured by the network. Vectors are all same length, but are color-coded by their rate. Stars are the locations of the stations used for the Euler pole estimation (Table 2), which yields a result nearly identical to the net-rotation pole.*

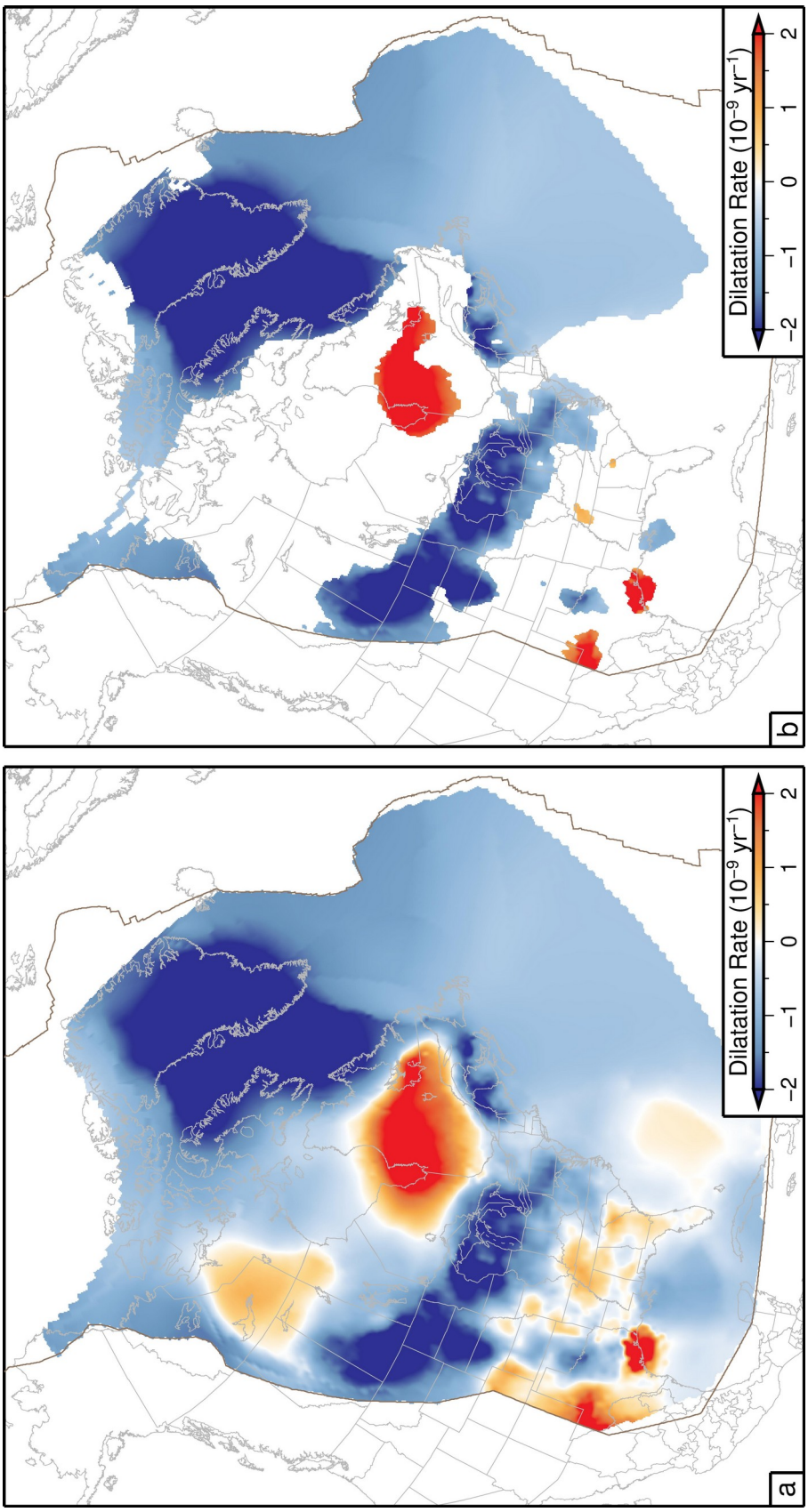

Figure 3 *– Dilatational strain rate field associated with the intraplate deformation. Negative (blue) is contraction, positive (red) is extension. a) all, b) where signal>2σ.*

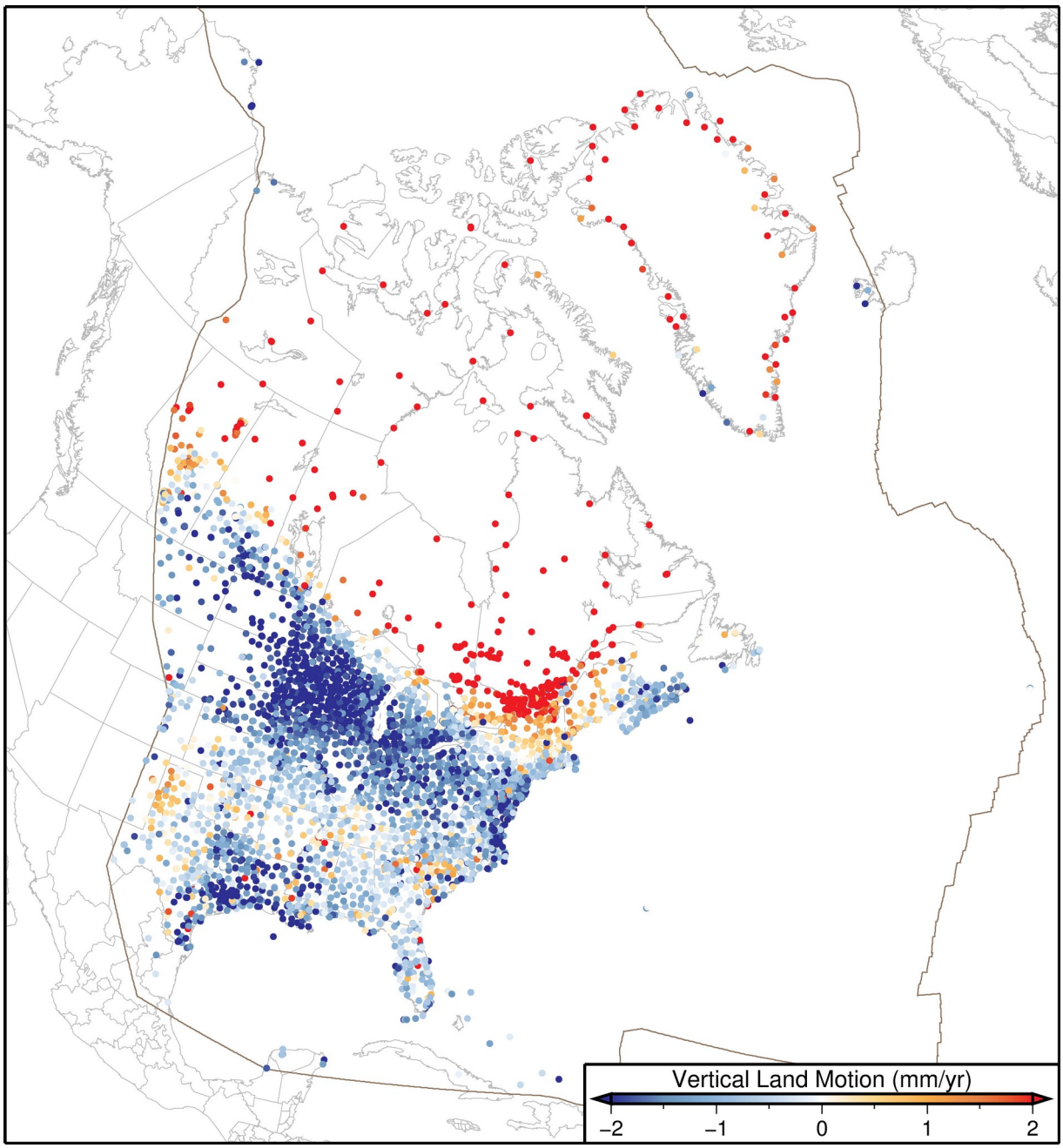

Figure 4 *– Vertical land motion (color scale is saturated at ±2 mm/yr).*

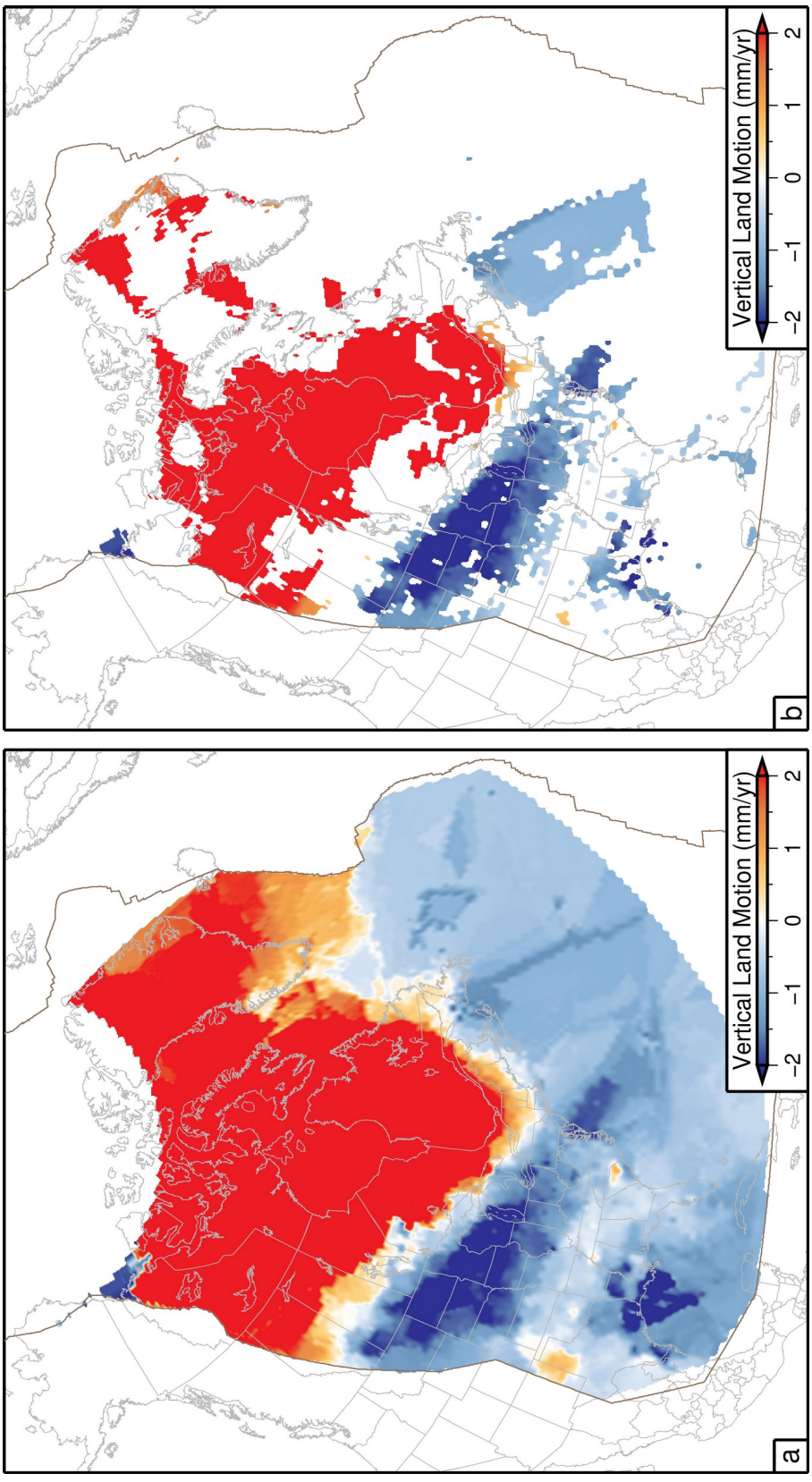

Figure 5 *– Imaged vertical land motion (color scale is saturated at ±2 mm/yr). a) all, b) where signal>2σ.*